ENSO Modulation: Is It Decadally Predictable?

ANDREW T. WITTENBERG, ANTHONY ROSATI, THOMAS L. DELWORTH, GABRIEL A. VECCHI, AND FANRONG ZENG

NOAA/Geophysical Fluid Dynamics Laboratory, Princeton, New Jersey

(Manuscript received 24 September 2013, in final form 12 December 2013)

ABSTRACT

Observations and climate simulations exhibit epochs of extreme El Niño–Southern Oscillation (ENSO) behavior that can persist for decades. Previous studies have revealed a wide range of ENSO responses to forcings from greenhouse gases, aerosols, and orbital variations, but they have also shown that interdecadal modulation of ENSO can arise even without such forcings. The present study examines the predictability of this intrinsically generated component of ENSO modulation, using a 4000-yr unforced control run from a global coupled GCM [GFDL Climate Model, version 2.1 (CM2.1)] with a fairly realistic representation of ENSO. Extreme ENSO epochs from the unforced simulation are reforecast using the same (''perfect'') model but slightly perturbed initial conditions. These 40-member reforecast ensembles display potential predictability of the ENSO trajectory, extending up to several years ahead. However, no decadal-scale predictability of ENSO behavior is found. This indicates that multidecadal epochs of extreme ENSO behavior can arise not only intrinsically but also delicately and entirely at random. Previous work had shown that CM2.1 generates strong, reasonably realistic, decadally predictable high-latitude climate signals, as well as tropical and extratropical decadal signals that interact with ENSO. However, those slow variations appear not to lend significant decadal predictability to this model's ENSO behavior, at least in the absence of external forcings. While the potential implications of these results are sobering for decadal predictability, they also offer an expedited approach to model evaluation and development, in which large ensembles of short runs are executed in parallel, to quickly and robustly evaluate simulations of ENSO. Further implications are discussed for decadal prediction, attribution of past and future ENSO variations, and societal vulnerability.

1. Introduction

The El Niño–Southern Oscillation (ENSO) phenomenon is a primary player in global climate, driving remote teleconnections that affect weather, ecosystems, and economies worldwide (Clarke 2008; Sarachik and Cane 2010). Historical observations, paleo proxy records, and numerical simulations indicate that ENSO behavior is modulated from decade to decade (Wittenberg 2009; Vecchi and Wittenberg 2010; Li et al. 2011, 2013; Emile-Geay et al. 2013a,b; McGregor et al. 2013). Going forward, an important question is whether the coming decades will bring a barrage of strong ENSO events or none at all.

ENSO modulation may be partly intrinsic, arising from chaotic and/or stochastically driven tropical Pacific dynamics (Kleeman and Power 1994; Blanke et al. 1997; Timmermann et al. 2003; Jochum and Murtugudde 2004; Flügel et al. 2004; Yeh et al. 2004; Power and Colman 2006; Vecchi et al. 2006b; Gebbie et al. 2007; Zavala-Garay et al. 2008; Kleeman 2008; Wittenberg 2009; Newman et al. 2011a,b). ENSO may also be modulated by slow changes in background climate, arising from ENSO nonlinearities, non-ENSO climate modes, or natural and anthropogenic radiative forcings (Kirtman and Schopf 1998; Wang and An 2001, 2002; Wittenberg 2002; Zhang and DeWitt 2006; Moon et al. 2007; An et al. 2008; Matei et al. 2008; Anderson et al. 2009; Imada and Kimoto 2009; DiNezio et al. 2012; Ogata et al. 2013). These mechanisms are compatible, and indeed existing observational records are not yet sufficient to rule out the possibility of a stochastically driven, chaotic ENSO perturbed by both non-ENSO climate modes and external forcings (Chang et al. 1996; Penland et al. 2000; Zhang et al. 2003; Fedorov et al. 2003; Flügel et al. 2004; Kravtsov 2012).

Climate models from phases 3 (CMIP3) and 5 (CMIP5) of the Coupled Model Intercomparison Project suggest

Corresponding author address: Andrew T. Wittenberg, NOAA/GFDL, 201 Forrestal Rd., Princeton, NJ 08540-6649.
E-mail: andrew.wittenberg@noaa.gov

DOI: 10.1175/JCLI-D-13-00577.1

ambiguous impacts of anthropogenic forcings on ENSO sea surface temperature (SST) variability over the next several decades (van Oldenborgh et al. 2005; Guilyardi et al. 2009; Collins et al. 2010; Stevenson et al. 2012; Watanabe et al. 2012; Guilyardi et al. 2012a). These projections generally show a less than 50% change in ENSO SST anomaly (SSTA) amplitude arising from anthropogenic forcings over the next century, with ENSO SSTAs weakening in some models and strengthening in others. ENSO rainfall anomalies, in contrast, are projected to strengthen over the central Pacific in response to eastern equatorial Pacific warming (Vecchi and Wittenberg 2010; Watanabe et al. 2012; Cai et al. 2012, 2014). In many models, the intrinsic ENSO modulation is so large that anthropogenic changes in ENSO cannot be reliably detected over the next few decades, with only a single realization. It is therefore plausible that ENSO's behavior over the coming decades could be influenced as much by intrinsic modulation as by changes in radiative forcing.

The ability to accurately project ENSO behavior for the coming decades may then hinge on how long the ENSO system retains memory of its initial conditions. Observational and model analyses have seen little evidence for ENSO memory beyond a few years, with warm events occurring seemingly independent of each other (Larkin and Harrison 2002; Kessler 2002; Choi et al. 2013), except possibly for very strong events (Yukimoto and Kitamura 2003; Wittenberg 2009). Studies of ENSO predictability and forecast skill—primarily using intermediate-complexity dynamical and statistical models—suggest potential skill in predicting tropical Pacific SSTAs at lead times exceeding 1 year and possibly more than 2 years for some events (Penland and Sardeshmukh 1995; Knaff and Landsea 1997; Latif et al. 1998; Grötzner et al. 1999; Barnston et al. 1999; Collins and Allen 2002; Zhang et al. 2001; Mason and Mimmack 2002; Wang et al. 2002; Chen et al. 2004; Flügel et al. 2004; Jin et al. 2008; Luo et al. 2008; Tang et al. 2008).

Past coupled GCM (CGCM) studies of ENSO's potential predictability have used a "perfect model" approach, in which a particular model trajectory is reforecast using an ensemble of perturbed runs from the same model (Boer 2000; Collins et al. 2002; Collins 2002; Power et al. 2006). Those CGCM studies, however, could afford only small reforecast ensembles, the largest of which were the five-member ensembles initialized from twentieth-century simulations by Collins (2002). Unfortunately the small ensembles and changing radiative forcings in those studies hampered their diagnoses of ENSO predictability. To better probe the limits of ENSO predictability, here we capitalize on improved computational power by running large-ensemble reforecasts of extreme ENSO epochs, selected from a very long control run of a widely used CGCM with a fairly realistic ENSO simulation.

2. Methods

a. Coupled general circulation model

The model used for this study is the Geophysical Fluid Dynamics Laboratory (GFDL) Climate Model, version 2.1 (CM2.1), a global ocean–atmosphere–land–ice CGCM whose formulation and simulation characteristics have been extensively described (Delworth et al. 2006; Anderson et al. 2004; Griffies et al. 2005; Gnanadesikan et al. 2006; Wittenberg et al. 2006). The global, tropical, and ENSO simulations of CM2.1 all rank highly among CMIP3-class models (van Oldenborgh et al. 2005; Guilyardi 2006; Capotondi et al. 2006; Merryfield 2006; Joseph and Nigam 2006; Reichler and Kim 2008). CM2.1 simulates a broad diversity of ENSO "flavors" (Kug et al. 2010; Takahashi et al. 2011; Capotondi and Wittenberg 2013), including extreme El Niños and their distinct life cycle involving precursor westerly wind events (WWEs), development of an equatorial intertropical convergence zone (ITCZ), elimination of equatorial upwelling, and delayed event termination (Vecchi and Harrison 2006; Vecchi 2006; Lengaigne and Vecchi 2010).

CM2.1 is used routinely for seasonal-to-interannual forecasts and decadal-to-centennial climate projections (Stouffer et al. 2006; Zhang et al. 2007; Song et al. 2008; Wang et al. 2008; Xie et al. 2010; Knutson et al. 2013a,b; Yang et al. 2013; Vecchi et al. 2013; Msadek et al. 2013, manuscript submitted to *J. Climate*), so understanding the model's predictability may shed light on its performance in those contexts. While CM2.1 does have a fairly strong ENSO, among the CMIP3 and CMIP5 CGCMs it is not an outlier in terms of either its present-day ENSO amplitude or its change in tropical Pacific climate/ENSO induced by twenty-first-century anthropogenic forcings [see, e.g., Fig. 10.16 of Meehl et al. (2007)]. CM2.1 is also the parent of several new models recently developed by GFDL: the Climate Model version 2 with the Modular Ocean Model version 4p1 at coarse resolution (CM2Mc) (Galbraith et al. 2011), an Earth System Model with the Modular Ocean Model (ESM2M), an Earth System Model with the Generalized Ocean Layer Dynamics ocean model (ESM2G) (Dunne et al. 2012, 2013), CM3 (Donner et al. 2011; Griffies et al. 2011), CM2.5 and CM2.6 (Delworth et al. 2012), and the Forecast-Oriented Low Ocean Resolution (FLOR) version of CM2.5 (G. A. Vecchi et al. 2014, unpublished manuscript). Thus, insights gained from the present experiments could help illuminate the behavior of those other models as well.

CM2.1 captures many of the observed decadal-scale patterns of extratropical Pacific variability and their teleconnections to and from the tropics (Zhang et al. 2011; Furtado et al. 2011; Li and Lau 2012). CM2.1 also produces multidecadal oscillations of the Atlantic meridional overturning circulation (AMOC) and North Atlantic SSTs, which are decadally predictable to some extent (Msadek et al. 2010; Branstator et al. 2012; Yang et al. 2013), so it is worth exploring whether those decadal fluctuations lend any decadal predictability to the model's ENSO behavior.

Ogata et al. (2013) examined the relationship between tropical Pacific decadal variability and the decadal modulation of ENSO amplitude in CM2.1. Simulated strong ENSO epochs were found to be associated with a decadal-mean warming of eastern equatorial Pacific SST, cooling of western equatorial Pacific SST, and vertical expansion of the equatorial thermocline. These decadal effects were found to be largely associated with ENSO-induced temporal ''blurring'' of the tropical Pacific thermal structure (Schopf and Burgman 2006), rather than systematic changes in the instantaneous ocean thermal gradients, suggesting that the ENSO modulation caused the decadal-scale changes and not vice versa. Ogata et al. (2013) then hypothesized a coupled feedback mechanism, whereby residual effects of ENSO modulation could rectify onto the decadal-mean state, altering ENSO stability and contributing to persistent epochs of extreme ENSO behavior. The present study tests whether such a feedback mechanism, if it exists, imparts any decadal predictability to CM2.1's unforced ENSO behavior.

b. 4000-yr reference control run

We begin with a long preindustrial control simulation of CM2.1, which is an extension of the 2000-yr run described in Wittenberg (2009). This control run was initialized from twentieth-century conditions as in Delworth et al. (2006) and then run without flux adjustments for 4220 years, with fixed 1860 estimates of solar irradiance, land cover, and atmospheric composition. The spinup over the first 220 years is discarded, and only the subsequent 4000 years (denoted as years 0001–4000) are analyzed.

The control run produces a stable surface climatology, with very little climate drift of the tropical Pacific upper ocean and atmosphere. SSTs averaged over the Niño-3 region (5°S–5°N, 150°–90°W) warm by only 0.12°C from the first millennium to the second and by 0.05°C from the second millennium to the third. This small drift is isolated by smoothing the monthly-mean time series $T_{\rm tot}$ with a 2125-month triangle that transmits 25%, 50%, and 75% of the amplitude at periods of 147, 200, and 304 years. The resulting low-pass-filtered time series is then subtracted from $T_{\rm tot}$ to yield a high-pass-filtered, detrended temperature time series T. A 12-month climatology is then removed from T, resulting in the monthly-mean SSTAs T' to be analyzed.

c. Extreme ENSO epochs

The control simulation spontaneously produces epochs of extreme ENSO behavior, which can last for decades or even centuries. Figure 1 shows three such epochs in the 4000-yr control run, labeled as M7, M2, and M5, as in Wittenberg (2009). Epoch M7 loosely resembles the observed behavior of ENSO in the 1980s and late 1990s, with strong, warm-skewed events 5 or more years apart, strong phase locking of the warm peaks to the end of the calendar year, strong zonal displacement between the SSTA patterns of cold and warm events, and clear eastward-propagating features during the transitions from warm to cold events (Lengaigne and Vecchi 2010; Takahashi et al. 2011). Epoch M2 exhibits moderate-amplitude, frequent, regularly spaced ENSO events and more warm/cold symmetry than in M7, resembling the observed behavior during the 1960s and 1970s (Wang 1995; Wang and An 2002). Epoch M5 exhibits mainly weak, biennial variability near the dateline, much like the early 1990s and 2000s (Yeh et al. 2009).

We have selected these three epochs because of their unusual amplitude, frequency, skewness, and/or regularity in terms of Niño-3 SSTA, an index that is strongly linked (though often nonlinearly) to other important ENSO indices, including various tropical Pacific SSTA patterns (Takahashi et al. 2011), equatorial Pacific rainfall (Lengaigne and Vecchi 2010; Watanabe and Wittenberg 2012; Watanabe et al. 2012; Cai et al. 2014), the Southern Oscillation index (SOI) based on sea level pressure gradients (Chiodi and Harrison 2013), and numerous other impacts around the globe. We defer exploration of those other indices and their epochal predictability for a future study.

d. Ensemble reforecasts

The extreme ENSO epochs of Fig. 1 are then reforecast using the same model executable and computing platform that generated the original control run, which we shall refer to as the ''reference run.'' Arrows in Fig. 1 highlight the nine initialization times. At 1 January of years 1721, 1731, and 1741 (epoch M7); 541, 551, and 561 (epoch M2); and 1151, 1161, and 1171 (epoch M5), the simulated climate state is copied exactly from the reference run, except that a tiny perturbation δ_k is added to the temperature at one ocean grid cell. For each ensemble member $k = 1, \ldots, N$,

$$\delta_k = 0.0001^\circ\mathrm{C} \times \begin{cases} (k+1)/2: & \text{for odd } k \\ -k/2: & \text{for even } k \end{cases}. \qquad (1)$$

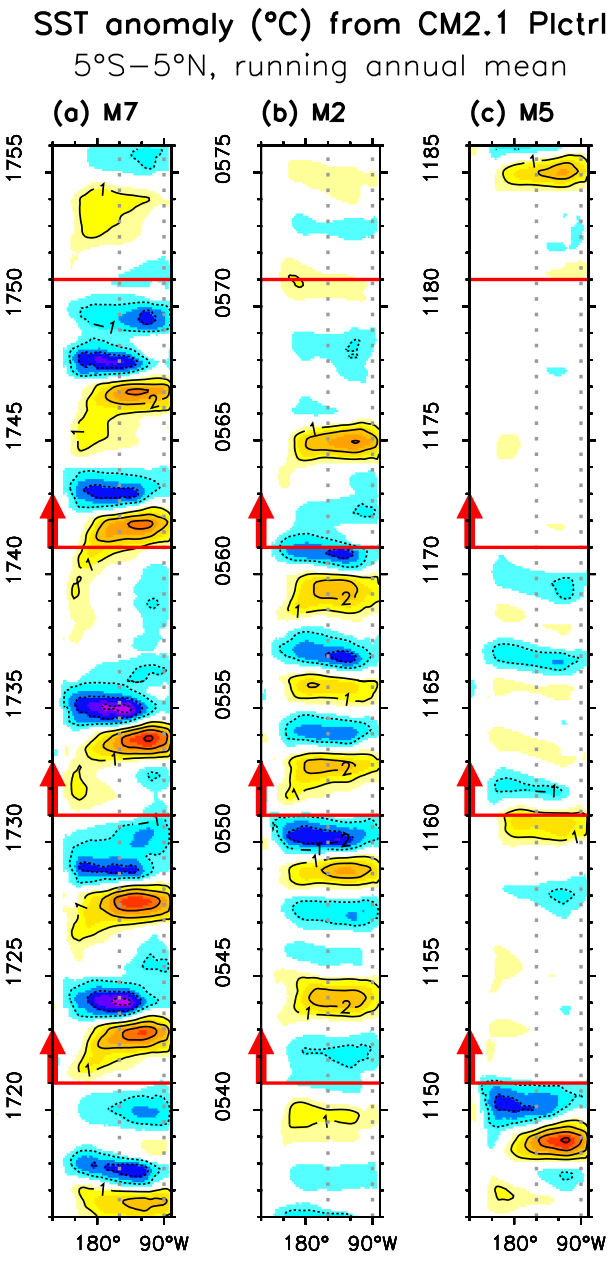

FIG. 1. Lon–time plot of SSTAs (°C) simulated in the CM2.1 control run, averaged 5°S–5°N over the Pacific for (a) a strong ENSO epoch, (b) a moderate and fairly steady ENSO epoch, and (c) a weak ENSO epoch. These correspond to epochs M7, M2, and M5 of Wittenberg (2009). The contour interval is 1°C, with shading incremented every half contour, and the zero contour is omitted. SSTAs are computed as running annual-mean SST departures from a multidecadal background state, where the latter is obtained via a 20-yr triangle smoother that transmits 25%, 50%, and 75% amplitude at periods of 17, 23, and 34 years. Dotted vertical lines enclose the Niño-3 region (150°–90°W), and red horizontal lines and arrows highlight the reforecast start/end times.

The N-member ensemble is then integrated forward in time for 10 years. As an initial check, we confirmed experimentally that a run with $\delta = 0$ duplicated the reference run, bitwise.

To help resolve the extremes of the forecast probability density function (PDF), an ensemble size of $N = 40$ is chosen so that at any given time, two members will lie above the 0.95 quantile of the forecast ensemble PDF and two members will lie below the 0.05 quantile. The δ_k are applied to the single ocean grid cell at 0.167°N, 179.5°E and 5-m depth. This cell spans 0.33° of latitude, 1° of longitude, and 10-m depth, representing a seawater volume of $4.1 \times 10^{10}\,\mathrm{m}^3$. Assuming a seawater density of $1023\,\mathrm{kg\,m}^{-3}$ and a specific heat capacity of 4.0 kJ (kg K)$^{-1}$, a δ_1 of magnitude 0.0001°C corresponds to an energy input of 17 TJ. This is a trivial energy increment for the climate system; a typical hurricane releases that much latent heat in 0.2 s (Emanuel 1999).

The initial perturbations are deliberately chosen to be infinitesimal as far as the model is concerned, near the level of rounding errors. This gives the reforecasts their best chance of reproducing the extreme ENSO epochs seen in the reference run, and permits assessment of the outer limits of the model's intrinsic predictability. Given a finite computer, these are the best conceivable forecasts of this model's climate system.

Over the first several hours of the reforecast, the GCM discretizations rapidly spread rounding errors to neighboring grid cells with each successive time step, so that tiny errors permeate the entire global CGCM state vector after just 1 day. This effectively removes any sensitivity to the precise structure of the initial perturbation, and allows subsequent error growth to arise organically out of the model dynamics. We find that amplifying the perturbation 10-fold, or instead applying it to a cell in the North Atlantic or at the bottom of the ocean, has no discernible effect on the statistics of global or local error growth beyond the first few days.

For SSTAs, the strongest growth of root-mean-square (RMS) ensemble spread is in midlatitude regions affected by strong local instabilities (e.g., in the vicinity of the atmospheric storm tracks, and near western boundary currents like the Kuroshio and Gulf Stream). The RMS spread of Niño-3 SSTA grows rapidly at first, approaching 0.1°C by month 4 of the forecast, with slower growth in subsequent months [see Fig. 5 of Karamperidou et al. (2013)]. Thus, for the purpose of assessing decadal predictability in this model, there is apparently no long-term difference between perturbing with errors at the level of rounding, versus at the level of real-world observations; that difference is effectively overcome after just a few months of integration.

Before analyzing the resulting reforecast SSTAs, the slowly evolving control-run trend (from section 2b) and

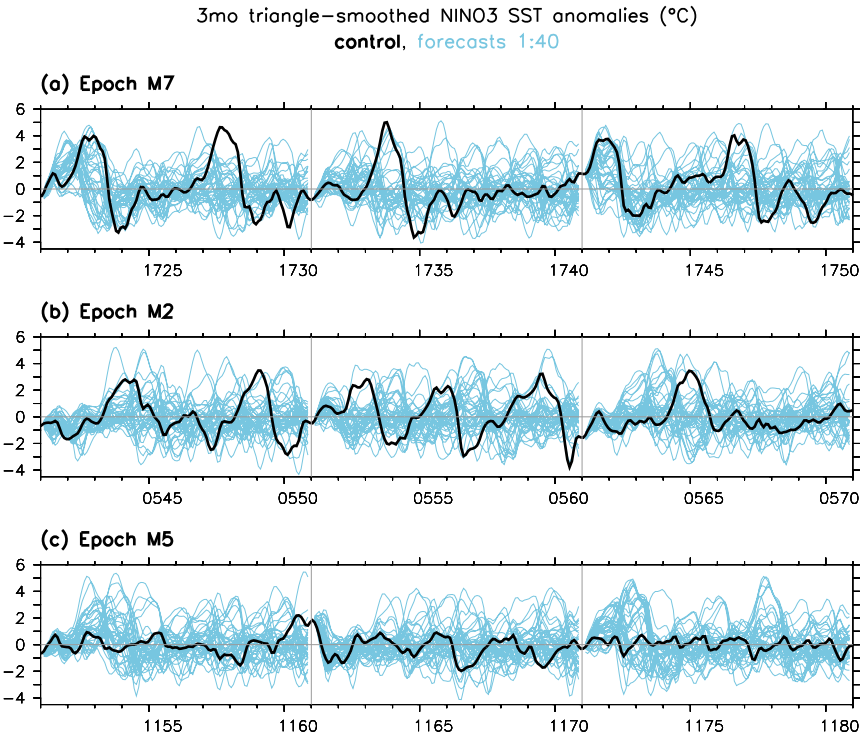

FIG. 2. CM2.1-simulated time series of smoothed SST anomalies (T'_s; °C) averaged over the Niño-3 region (5°S–5°N, 150°–90°W) during epochs (a) M7, (b) M2, and (c) M5. The reference control run (black) and its 40-member perfect-model reforecasts (blue) are shown. Gray vertical lines and left/right edges of plot indicate the reforecast start/end times.

the reference climatology are removed from all of the reforecasts. All time series T' are then smoothed with a 3-month triangle, which transmits 25%, 50%, and 75% amplitude at periods of 3.3, 4.5, and 6.9 months, resulting in a smoothed anomaly time series T'_s.

3. Results

a. Predictability of Niño-3 SSTA trajectories

Figure 2 shows the evolution of Niño-3 SSTAs in the CM2.1 reference run and reforecasts, for the three extreme ENSO epochs of Fig. 1. The 40-member reforecasts, at first tightly packed around the reference trajectory, gradually diverge over the next few years. Some reforecasts track the reference run for the entire decade, while others soon differ substantially from the reference. There is no apparent relationship (−0.06 correlation) between the magnitude of the initial δ_k, and a reforecast's subsequent Niño-3 SSTA RMS (across all 120 months) difference from the reference trajectory.

That even infinitesimal perturbations disrupt the control run's extreme ENSO epochs shows that these epochs were simply statistical flukes. In the unforced CM2.1, a flap of the butterfly's wings can extinguish a 30-yr epoch of strong ENSO events, disrupt a monotonous ENSO epoch, or create intense ENSO events where there would have been none before.

To quantify the predictability of Niño-3 SSTAs, the PDF of each reforecast ensemble must be compared against the climatological PDF of the full 4000-yr reference run. To summarize the reforecast PDFs from Fig. 2, we use their 0.05, 0.50, and 0.95 quantiles, indicated with blue lines in Fig. 3. At any given forecast lead, there is potential predictability when these reforecast quantiles are statistically distinct from the climatological quantiles. Specifically, for a finite forecast ensemble (here 40 members), the question is whether the reforecast quantiles exceed the range (induced by sampling variability) of the climatological quantiles for an ensemble of that size. We use the reference run to estimate that sampling range, for each of the three quantiles (gray bands in Fig. 3). For example, the bottom gray band for the 0.05 quantile in each panel of Fig. 3 is computed as follows:

(i) 40 decades are selected at random from the 4000-yr reference run, mimicking a 40-member forecast ensemble with no memory of its initial conditions;
(ii) the 0.05 quantile (5th percentile) is computed from this 40-member ensemble;

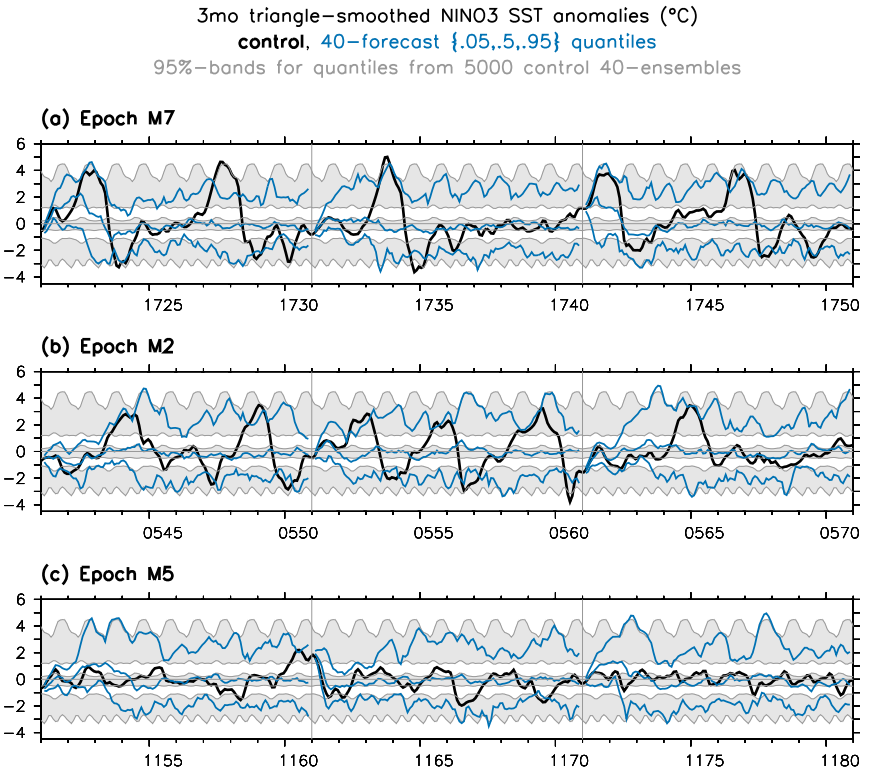

FIG. 3. As in Fig. 2, but with the reforecasts summarized by their 0.05, 0.50, and 0.95 quantiles (bottom, middle, and top blue lines). Gray bands indicate the range of sampling variability for those quantiles, based on similarly sized ensembles with no knowledge of the actual initial conditions for the forecast. For example, the bottom gray band in each panel indicates the central 95% sampling range for the distribution of 0.05 quantiles, computed from 5000 sets of 40 randomly selected decades (each starting with a January) from the 4000-yr reference run.

(iii) steps (i) and (ii) are repeated 5000 times; and
(iv) for the resulting distribution of 0.05 quantiles, the 95% range (2.5%–97.5%) is plotted as the bottom gray band.

The gray bands of sampling variability expand and contract seasonally, because of the seasonal synchronization of ENSO SSTA variance in CM2.1 [see, e.g., Fig. 22 of Wittenberg et al. (2006)]. For an ensemble with no memory of its initial conditions, one would expect only about 5% (binomially distributed) of its reforecast quantiles to fall outside the gray climatological bands. If exceedances occurred significantly more often than that, it would suggest that some initial-condition memory had been retained and that the Niño-3 SSTA trajectory might be potentially predictable.

Figure 3 shows that, 3–4 years after perturbation, the ensemble quantiles generally settle into their climatological ranges—indicating little predictability of the Niño-3 SSTA trajectory beyond interannual scales, even for the particularly extreme ENSO epochs selected here. A possible exception is the case initialized in year 1171, which shows an enhanced risk of warm events peaking near the ends of years 1172 and 1177. However, while both of those temporal peaks in the reforecast 0.95 quantile are somewhat significant at the two-sided 5% level, they are also ironic—the corresponding reference-run epoch (which was intentionally selected for its *inactivity*) showed no warming in either year 1172 or 1177 or indeed in any ENSO events at all during years 1171–80.

b. Predictability of ENSO's decadal amplitude

We now turn to the predictability of ENSO's decadal statistics. In particular we examine ENSO amplitude, defined here as $\overline{|T_s'|}$, a multiyear running mean of the absolute value of smoothed SSTAs. We are interested in whether the ENSO amplitude from the reference-run epochs is captured by the perturbed reforecasts, beyond the horizon of "trajectory predictability" seen in Fig. 3.

Figure 4 at first seems to offer some limited evidence for extended predictability of ENSO amplitude, over leads of 1–10 years (i.e., omitting only the first year of the forecast). Under a null hypothesis H_0 of zero

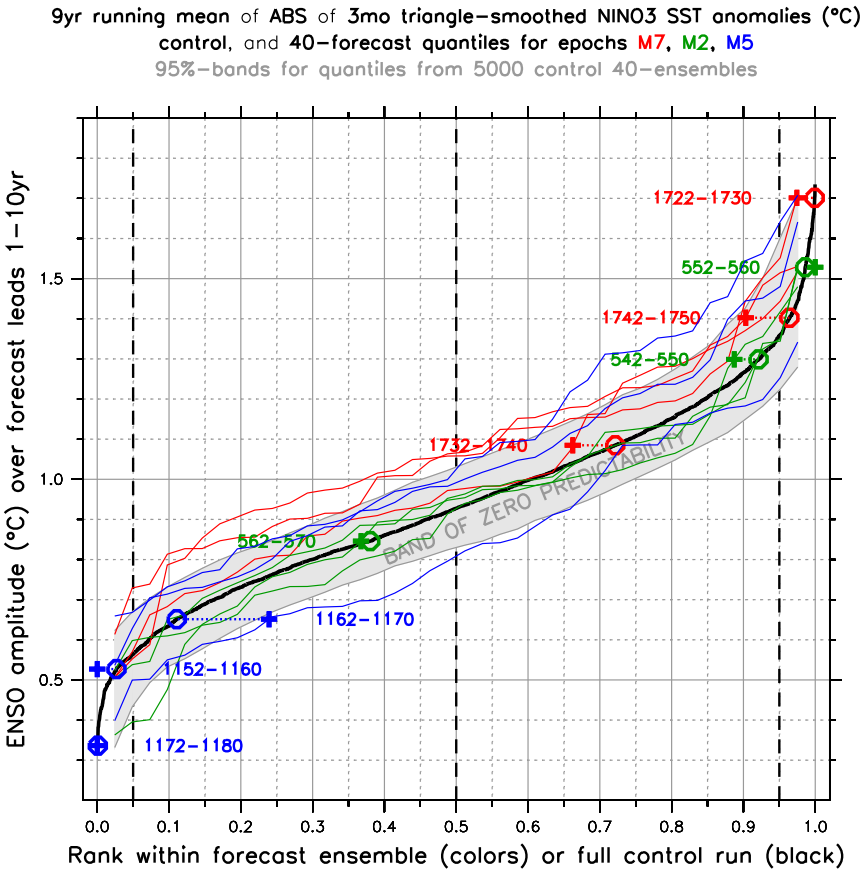

FIG. 4. CM2.1 distributions of ENSO amplitude ($\overline{|T_s'|}$) over forecast leads of 1–10 years. Ordinate gives the amplitude, and abscissa gives the rank (quantile) of that amplitude either within the 40-member reforecasts (colored curves) or within the set of all 9-yr chunks from the 4000-yr reference run (black curve). Each reforecast curve is color coded by epoch (M7 is red, M2 is green, and M5 is blue). For each case, the target amplitude from the reference run is indicated with a year-range label, plus a horizontal dotted line that intersects the rank of that amplitude within the reforecast ensemble (cross) and within the reference run (circle). The gray "band of zero predictability" indicates the 95% range for quantiles from 40-member ensembles selected at random from the reference run (as in Fig. 3), which are entirely ignorant of the correct initial conditions for any forecast.

predictability of ENSO amplitude, about 5% (binomially distributed) of the colored reforecast curves would be expected to exceed the vertical span of the gray "band of zero predictability," which attends the climatological distribution of 9-yr ENSO amplitudes (black line) from the 4000-yr reference run. Several of the reforecast quantiles significantly (but not strongly) exceed that amplitude range. For two of the reforecasts of the active M7 epoch (red lines for years 1722–30 and 1742–50, extending above the gray band), the weakest-amplitude members of the ensemble are not quite as weak as would have been expected from H_0. For one of the reforecasts of the quiet M5 epoch (blue line for years 1162–70, extending below the gray band) the weakest-amplitude members are somewhat weaker than would have been expected from H_0. Ironically though, the reforecast for the quietest M5 epoch (blue line for years 1172–80, extending above the gray band) shows significantly stronger than expected amplitudes for its strongest-amplitude members, suggesting that the quietness of the reference run during these years was a statistical fluke. In Fig. 4, the circle and cross confirm that the reference run's behavior for years 1172–80 was a very rare event—not just with respect to the 4000-yr control, but even with respect to perfect-model reforecasts with nearly perfect initial conditions. For the fairly strong and monotonous M2 epoch, the amplitude reforecasts are not statistically distinct from H_0 at any quantile, apart from years 562–70, which have slightly weaker low-end quantiles than would have been expected from H_0. Interestingly, in every case

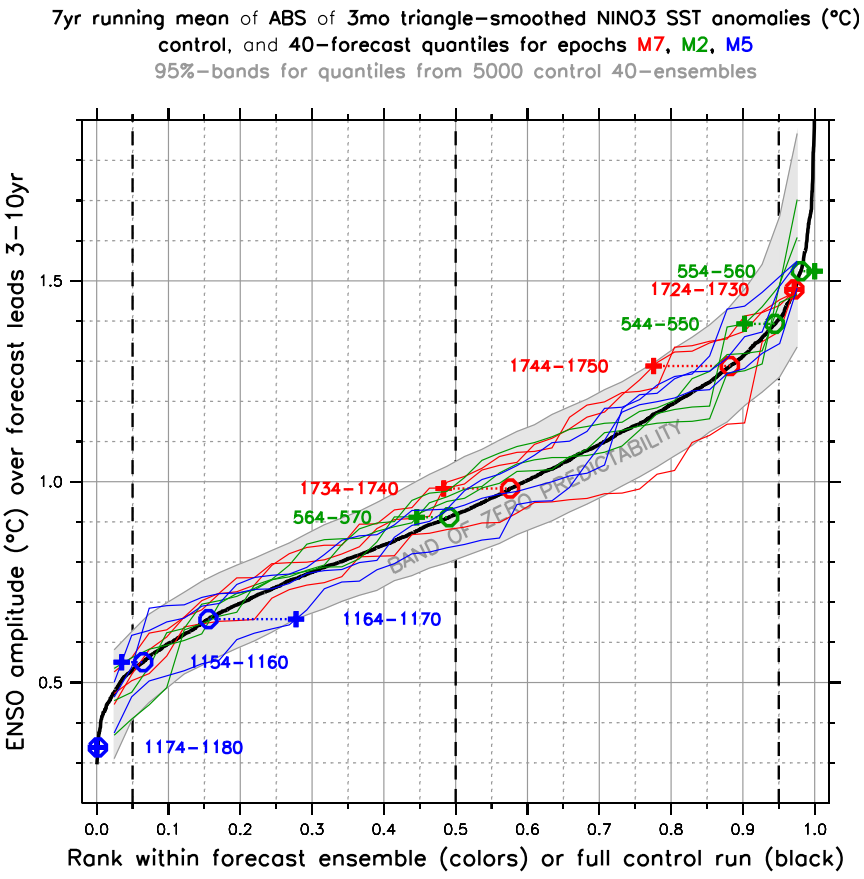

FIG. 5. As in Fig. 4, but for forecast ENSO amplitudes over leads of 3–10 years.

examined here, the rank of the reference run within the reforecast PDF (cross) is within 0.15 of its rank within the climatological PDF (circle). Furthermore, in only five of the nine cases is the reference run's rank within the reforecast PDF less extreme than within the climatological PDF. This suggests that, for predicting the model's mean ENSO amplitude over lead times of 1–10 years, "initial-condition ignorant" climatological statistics would have been a good proxy for the initialized ensemble reforecasts.

To emphasize this point, we next omit the first 3 years of each forecast before computing the multiyear ENSO amplitude. Figure 5 shows that, consistent with H_0 at these longer leads, essentially none of the reforecast distributions of ENSO amplitude are statistically distinct from the climatological distribution at any quantile. The weak epoch (blue) reforecast curves as a group are not statistically distinct from the strong epoch (red and green) curves. The one exception (red curve extending slightly below the gray band) is again ironic: during years 1724–30 the reforecasts showed a somewhat weaker than average ENSO, with reduced probability of a high-amplitude epoch, but during that time the reference-run ENSO was particularly strong, at the extreme end of both the reforecast and climatological distributions. Indeed for the cases examined here, all of the reference run's strong ENSO decades (circles to the right of the 0.8 quantile) and weak ENSO decades (circles to the left of the 0.2 quantile) were on the extreme ends of both their reforecast PDFs and the climatological PDF, and in only four of the nine cases was the reference's quantile within the reforecast PDF less extreme than within the climatological PDF. It thus appears that the limited predictability of amplitude seen at leads of 1–10 years (Fig. 4) arose from just the first 2–3 years of the forecasts.

For the model and epochs examined here, it is clear that even a very tiny perturbation can randomize ENSO's decadal amplitude after just a few years. In the absence of external forcings, no evidence is found for decadal predictability of this model's ENSO statistics, beyond the information contained in its climatological PDF.

4. Discussion

a. *Implications*

Wittenberg (2009) posed a null hypothesis (H_0) that, in the absence of external forcings, the decadal statistics

of ENSO's modulation are consistent with those of a memoryless (Poisson) process with an interannual time scale. Just as flipping a fair coin can sometimes produce a long run of heads, a random interannual process can occasionally generate extreme multidecadal epochs. Analyzing the wait times between moderate to strong ENSO events, Wittenberg (2009) was unable to rule out H_0 for the CM2.1 control run on decadal scales. The present study lends even more support to H_0, by demonstrating that the decadal statistics of CM2.1's most extreme ENSO epochs are essentially unpredictable. If ENSO's real-world behavior over the next few decades is likewise indistinguishable from nature's climatological PDF, then assessing societal vulnerability in the near term will rely on accurately characterizing that climatological PDF—using instrumental records, paleo proxies, and simulations from a diverse set of models.

The predictability of ENSO modulation bears not only on prospects for decadal forecasts of ENSO but also on decadal predictability of other phenomena—ENSO modulation is known to rectify into decadal and longer time scales (Flügel and Chang 1999; Newman et al. 2003; Rodgers et al. 2004; An 2004; Yeh and Kirtman 2005; Cibot et al. 2005; Schopf and Burgman 2006; Watanabe and Wittenberg 2012; Watanabe et al. 2012; Ogata et al. 2013). This is a pressing issue, because the climate community has invested heavily in initialized decadal climate projections, in hopes that these might be more skillful than uninitialized projections (Taylor et al. 2012). If intrinsic ENSO modulation were indeed unpredictable, then it would act as stochastic forcing for slower climate modes, potentially limiting their predictability as well. ''ENSO noise'' must therefore be considered in investigations of decadal variability and predictability, including attributions of past variations and assessments of future anthropogenic influence (e.g., Vecchi et al. 2006a; Power and Colman 2006; McPhaden et al. 2011; Solomon and Newman 2011; Newman 2013; Kosaka and Xie 2013).

As mentioned in section 2a, CM2.1 exhibits robust and predictable decadal climate variations in the extratropics, as well as decadal climate signals in the tropics that are linked with ENSO. Previous studies have suggested that the Atlantic multidecadal oscillation (AMO) may be decadally predictable (Smith et al. 2007; Keenlyside et al. 2008; Msadek et al. 2010; Yang et al. 2013; Vecchi et al. 2013; Msadek et al. 2013, manuscript submitted to *J. Climate*) and could influence the tropical Pacific climatology and thereby ENSO (Zhang and Delworth 2005; Dong et al. 2006; Dong and Sutton 2007; Timmermann et al. 2007). The AMO is thought to fluctuate with a characteristic time scale of approximately 40–100 years, although observational and paleo records are not yet sufficient to fully characterize the real-world AMO spectrum, and the drivers of recent Atlantic SST fluctuations are being actively debated (Frankcombe et al. 2010; Booth et al. 2012; Zhang et al. 2013; Cheng et al. 2013). CM2.1 reproduces the broad spatial pattern of the observed AMO, but it has a shorter dominant time scale of around 20 years, and like many CGCMs its associated SSTA variability is weaker than observed in the tropical Atlantic and stronger than observed in the North Atlantic subpolar gyre (Msadek et al. 2010; Ting et al. 2011; Zhang and Wang 2013; Msadek et al. 2013, manuscript submitted to *J. Climate*). CM2.1's AMO is predictable at lead times of up to a decade, although its amplitude, regularity, and predictability are modulated with time (Msadek et al. 2010; Branstator et al. 2012; Yang et al. 2013).

Zhang and Delworth (2005) showed that, when Atlantic SST changes are *imposed* in CM2.1—through an imposed North Atlantic freshwater forcing—those Atlantic changes could in turn cause decadal meridional shifts in the tropical Pacific ITCZ, via an atmospheric bridge over Central America. Subsequent model studies also found Atlantic-induced changes in the Pacific ITCZ (Dong et al. 2006; Dong and Sutton 2007; Timmermann et al. 2007), but the impacts on ENSO depended on the model formulation and the form of the imposed Atlantic forcing (Timmermann et al. 2007; Rashid et al. 2010; Svendsen et al. 2013). In the fully coupled system, decadal variations in Atlantic SSTs could themselves be driven partly by Pacific variability (e.g., ENSO), and a number of interbasin feedback loops have been suggested. Whatever the nature of these decadal interactions, the present study suggests (at least in the unforced CM2.1) that any such mechanisms are too weak and/or too unpredictable to impart robust decadal predictability to the statistics of ENSO.

Several studies have proposed interdecadal feedback loops, whereby ENSO modulation alters the decadal background climate, which then alters the dynamics of ENSO—leading to prolonged epochs of extreme ENSO behavior (Sun and Zhang 2006; Dewitte et al. 2007; Choi et al. 2009; Ogata et al. 2013). The present study indicates that, in CM2.1 at least, any such intrinsic decadal feedbacks are too weak to lend decadal predictability to ENSO, or to explain ENSO's interdecadal modulation. Note that decadal feedback loops (or forcings from decadal modes) are not actually necessary to produce decadal modulation of ENSO, which can arise even from a purely memoryless process with an interannual time scale (Wittenberg 2009). Of course, the real-world ENSO could also be affected by external (e.g., anthropogenic, volcanic, or solar) forcings, and our results in no way dismiss those effects. However, strong and decadally unpredictable ENSO modulation could pose challenges for *detecting* those forced effects, in the face

of short observational records influenced by changing observing systems.

b. Caveats

While a lack of decadal predictability for intrinsic ENSO modulation (as suggested by these experiments) could be viewed as disappointing, it is somewhat encouraging that ENSO behavior might sometimes be predictable several years in advance. *Realizing* that potential predictability in actual forecasts, however, will likely remain a challenge—because of imperfections in observations, models, and data assimilation systems, which lead to systematic biases and other forecast errors (Wittenberg 2004; Zhang et al. 2005, 2007; Sun et al. 2007; Guilyardi et al. 2012b; Goddard et al. 2013). In addition, the predictability of ENSO's various impacts (e.g., on rainfall over the United States) will no doubt be less than for Niño-3 SSTA, owing to interference from non-ENSO climate modes and weather noise.

Our experiments indicate that the prospects for decadal predictability of tropical Pacific variability, arising from initialization of the ''internal variability'' component of climate, may be limited. However, changes in radiative forcing—arising in part from increasing greenhouse gases—may provide a source of multidecadal predictability for ENSO statistics. It has been suggested that increasing greenhouse gases may favor a westward shift in the longitude of peak SSTAs during El Niño events (Yeh et al. 2009) and may increase the severity of ENSO-induced tropical precipitation anomalies (Boer 2009; Vecchi and Wittenberg 2010; Watanabe et al. 2012; Cai et al. 2012, 2014). Nevertheless, our results suggest that expectations should be set low for additional decadal refinement through *initialization* of multidecadal projections of future ENSO statistics.

CM2.1's intrinsic ENSO predictability could certainly differ from that of the real world. If the model underestimates intrinsic decadal modes of variability (e.g., in the North Pacific, North Atlantic, or Southern Ocean) and/or their effects on ENSO, then the predictability of its intrinsic ENSO modulation could be too low. CM2.1's ENSO is stronger than observed, which could either enhance its predictability (by helping its ENSO signals to stand out against background noise) or reduce it (if the overly strong ENSO is too nonlinear and chaotic). Karamperidou et al. (2013) suggest that, at least for 4-month lead times, trajectories of Niño-3 SSTA near-neighbor analogs tend to diverge more rapidly in CM2.1 than observations, so it is conceivable that multiyear ENSO predictability could be similarly underestimated by CM2.1. Our reforecast experiments should thus be repeated with other models, to evaluate the robustness of these results.

There may be epochs of the CM2.1 control run with longer or shorter windows of predictability than the three extreme ENSO epochs analyzed here. In particular, it is conceivable that predictability could be extended following an extreme El Niño (Goddard and Dilley 2005), as its aftermath reverberates through the climate system—for example, via climate signals induced in off-equatorial ocean heat content. On the other hand, the analysis of Karamperidou et al. (2013) suggests that CM2.1's Niño-3 SSTA error-growth rates, estimated from the divergence of nearest-neighbor analogs at 4-month leads, vary decadally by only 10%–20%.

c. A silver lining: Accelerated model evaluation

If it can be confirmed (at least in models) that ENSO's intrinsic memory is indeed limited to interannual scales, then there may be a silver lining: accelerated model evaluation and development. When comparing a model against observations or other models, several centuries of simulation may be required to characterize certain ENSO statistics (Wittenberg 2009; Stevenson et al. 2012; Deser et al. 2012; Borlace et al. 2013). However, a 100-yr simulation with a next-generation CGCM can take a month or longer—posing a major hindrance to model development, where sequences of many such evaluations are required.

If ENSO's memory is short, then an alternative could be to initialize an *ensemble* of model realizations from slightly perturbed initial conditions, as done here. For a model with no ENSO memory beyond 5 years, running 40 realizations for 40 years each (discarding the first 5 years) would produce a 1400-yr sample of ENSO behavior—35 times faster than a long serial run, with only 14% greater computational cost. If these ensemble runs were additionally driven with the time-evolving radiative forcings from a well-observed historical epoch (e.g., the 40 years span 1974–2013), it would be more straightforward to compare the simulation against the real-world ENSO—avoiding the pitfalls of basing these comparisons on preindustrial control simulations (where the forcings and observational targets are poorly known) or present-day control simulations (where the forcings are held fixed, leading to unrealistic rates of warming). In addition, the dispersion of the model ensemble during the ensemble-spinup period would help to illuminate the predictability of ENSO and other climate phenomena.

5. Summary

This study examined a 4000-yr preindustrial control simulation from a fairly realistic global coupled GCM, which exhibits intrinsically generated modulation of its ENSO behavior—producing epochs of extreme intensity, frequency, spatiotemporal patterns, and (ir)regularity

that last for decades. Ensemble reforecasts of this simulation's most extreme ENSO epochs, using a perfect model and near-perfect initial conditions, suggest occasional potential predictability of the control run's ENSO trajectory several years ahead. However, in the absence of external forcings, the reforecasts offer no evidence for predictability of decadal-scale ENSO statistics, beyond the information contained in the climatological PDF. While the potential implications of these results are sobering for decadal predictability, they also suggest an expedited approach to model evaluation and development, in which large ensembles of short runs are executed in parallel, to quickly and robustly assess a model's ENSO behavior.

The CM2.1 control run and its reforecasts represent a substantial computational investment: nearly 8000 years of simulation. We intend to use this unique dataset to further investigate the fundamental predictability of ENSO, as well as other climate phenomena.

Acknowledgments. We thank R. Msadek, X. Yang, and the three anonymous reviewers for their thoughtful and constructive comments.

REFERENCES

An, S.-I., 2004: Interdecadal changes in the El Niño–La Niña asymmetry. *Geophys. Res. Lett.,* **31,** L23210, doi:10.1029/2004GL021699.

——, J.-S. Kug, Y.-G. Ham, and I.-S. Kang, 2008: Successive modulation of ENSO to the future greenhouse warming. *J. Climate,* **21,** 3–21, doi:10.1175/2007JCLI1500.1.

Anderson, J. L., and Coauthors, 2004: The new GFDL global atmosphere and land model AM2/LM2: Evaluation with prescribed SST simulations. *J. Climate,* **17,** 4641–4673, doi:10.1175/JCLI-3223.1.

Anderson, W., A. Gnanadesikan, and A. Wittenberg, 2009: Regional impacts of ocean color on tropical Pacific variability. *Ocean Sci.,* **5,** 313–327, doi:10.5194/os-5-313-2009.

Barnston, A. G., M. H. Glantz, and Y. He, 1999: Predictive skill of statistical and dynamical climate models in SST forecasts during the 1997–98 El Niño episode and the 1998 La Niña onset. *Bull. Amer. Meteor. Soc.,* **80,** 217–243, doi:10.1175/1520-0477(1999)080<0217:PSOSAD>2.0.CO;2.

Blanke, B., J. D. Neelin, and D. Gutzler, 1997: Estimating the effect of stochastic wind stress forcing on ENSO irregularity. *J. Climate,* **10,** 1473–1486, doi:10.1175/1520-0442(1997)010<1473:ETEOSW>2.0.CO;2.

Boer, G. J., 2000: A study of atmosphere–ocean predictability on long time scales. *Climate Dyn.,* **16,** 469–477, doi:10.1007/s003820050340.

——, 2009: Changes in interannual variability and decadal potential predictability under global warming. *J. Climate,* **22,** 3098–3109, doi:10.1175/2008JCLI2835.1.

Booth, B. B. B., N. J. Dunstone, P. R. Halloran, T. Andrews, and N. Bellouin, 2012: Aerosols implicated as a prime driver of twentieth-century North Atlantic climate variability. *Nature,* **484,** 228–232, doi:10.1038/nature10946.

Borlace, S., W. Cai, and A. Santoso, 2013: Multidecadal ENSO amplitude variability in a 1000-yr simulation of a coupled global climate model: Implications for observed ENSO variability. *J. Climate*, **26,** 9399–9407, doi:10.1175/JCLI-D-13-00281.1.

Branstator, G., H. Teng, G. A. Meehl, M. Kimoto, J. R. Knight, M. Latif, and A. Rosati, 2012: Systematic estimates of initial-value decadal predictability for six AOGCMs. *J. Climate,* **25,** 1827–1846, doi:10.1175/JCLI-D-11-00227.1.

Cai, W., and Coauthors, 2012: More extreme swings of the South Pacific convergence zone due to greenhouse warming. *Nature,* **488,** 365–369, doi:10.1038/nature11358.

——, and Coauthors, 2014: Increasing frequency of extreme El Niño events due to greenhouse warming. *Nat. Climate Change,* **4,** 111–116, doi:10.1038/nclimate2100.

Capotondi, A., and A. Wittenberg, 2013: ENSO diversity in climate models. *U.S. CLIVAR Variations,* Vol. 11, No. 2, U.S. Climate Variability and Predictability Research Program, Washington, D.C., 10–14.

——, ——, and S. Masina, 2006: Spatial and temporal structure of tropical Pacific interannual variability in 20th century coupled simulations. *Ocean Modell.,* **15,** 274–298, doi:10.1016/j.ocemod.2006.02.004.

Chang, P., L. Ji, H. Li, and M. Flügel, 1996: Chaotic dynamics versus stochastic processes in El Niño–Southern Oscillation in coupled ocean–atmosphere models. *Physica D,* **98,** 301–320, doi:10.1016/0167-2789(96)00116-9.

Chen, J., M. A. Cane, A. Kaplan, S. E. Zebiak, and D. Huang, 2004: Predictability of El Niño over the past 148 years. *Nature,* **428,** 733–736, doi:10.1038/nature02439.

Cheng, W., J. C. H. Chiang, and D. Zhang, 2013: Atlantic meridional overturning circulation (AMOC) in CMIP5 models: RCP and historical simulations. *J. Climate,* **26,** 7187–7197, doi:10.1175/JCLI-D-12-00496.1.

Chiodi, A. M., and D. E. Harrison, 2013: El Niño impacts on seasonal U.S. atmospheric circulation, temperature, and precipitation anomalies: The OLR-event perspective. *J. Climate,* **26,** 822–837, doi:10.1175/JCLI-D-12-00097.1.

Choi, J., S.-I. An, B. Dewitte, and W. W. Hsieh, 2009: Interactive feedback between the tropical Pacific decadal oscillation and ENSO in a coupled general circulation model. *J. Climate,* **22,** 6597–6611, doi:10.1175/2009JCLI2782.1.

Choi, K., G. A. Vecchi, and A. T. Wittenberg, 2013: ENSO transition, duration, and amplitude asymmetries: Role of the nonlinear wind stress coupling in a conceptual model. *J. Climate,* **26,** 9462–9476, doi:10.1175/JCLI-D-13-00045.1.

Cibot, C., E. Maisonnave, L. Terray, and B. Dewitte, 2005: Mechanisms of tropical Pacific interannual-to-decadal variability in the ARPEGE/ORCA global coupled model. *Climate Dyn.,* **24,** 823–842, doi:10.1007/s00382-004-0513-y.

Clarke, A. J., 2008: *An Introduction to the Dynamics of El Niño and the Southern Oscillation.* Academic Press, 308 pp.

Collins, M., 2002: Climate predictability on interannual to decadal time scales: The initial value problem. *Climate Dyn.,* **19,** 671–692, doi:10.1007/s00382-002-0254-8.

——, and M. R. Allen, 2002: Assessing the relative roles of initial and boundary conditions in interannual to decadal climate predictability. *J. Climate,* **15,** 3104–3109, doi:10.1175/1520-0442(2002)015<3104:ATRROI>2.0.CO;2.

——, D. Frame, B. Sinha, and C. Wilson, 2002: How far ahead could we predict El Niño? *Geophys. Res. Lett.,* **29,** doi:10.1029/2001GL013919.

——, and Coauthors, 2010: The impact of global warming on the tropical Pacific and El Niño. *Nat. Geosci.,* **3,** 391–397, doi:10.1038/ngeo868.

Delworth, T. L., and Coauthors, 2006: GFDL's CM2 global coupled climate models. Part I: Formulation and simulation characteristics. *J. Climate,* **19,** 643–674, doi:10.1175/JCLI3629.1.

——, and Coauthors, 2012: Simulated climate and climate change in the GFDL CM2.5 high-resolution coupled climate model. *J. Climate,* **25,** 2755–2781, doi:10.1175/JCLI-D-11-00316.1.

Deser, C., and Coauthors, 2012: ENSO and Pacific decadal variability in the Community Climate System Model version 4. *J. Climate*, **25,** 2622–2651, doi:10.1175/JCLI-D-11-00301.1.

Dewitte, B., S.-W. Yeh, B.-K. Moon, C. Cibot, and L. Terray, 2007: Rectification of ENSO variability by interdecadal changes in the equatorial background mean state in a CGCM simulation. *J. Climate,* **20,** 2002–2021, doi:10.1175/JCLI4110.1.

DiNezio, P. N., B. P. Kirtman, A. C. Clement, S.-K. Lee, G. A. Vecchi, and A. Wittenberg, 2012: Mean climate controls on the simulated response of ENSO to increasing greenhouse gases. *J. Climate,* **25,** 7399–7420, doi:10.1175/JCLI-D-11-00494.1.

Dong, B., and R. T. Sutton, 2007: Enhancement of ENSO variability by a weakened Atlantic thermohaline circulation in a coupled GCM. *J. Climate,* **20,** 4920–4939, doi:10.1175/JCLI4284.1.

——, ——, and A. A. Scaife, 2006: Multidecadal modulation of El Niño–Southern Oscillation (ENSO) variance by Atlantic Ocean sea surface temperatures. *Geophys. Res. Lett.,* **33,** L08705, doi:10.1029/2006GL025766.

Donner, L. J., and Coauthors, 2011: The dynamical core, physical parameterizations, and basic simulation characteristics of the atmospheric component AM3 of the GFDL global coupled model CM3. *J. Climate,* **24,** 3484–3519, doi:10.1175/2011JCLI3955.1.

Dunne, J. P., and Coauthors, 2012: GFDL's ESM2 global coupled climate–carbon Earth system models. Part I: Physical formulation and baseline simulation characteristics. *J. Climate,* **25,** 6646–6665, doi:10.1175/JCLI-D-11-00560.1.

——, and Coauthors, 2013: GFDL's ESM2 global coupled climate–carbon Earth system models. Part II: Carbon system formulation and baseline simulation characteristics. *J. Climate,* **26,** 2247–2267, doi:10.1175/JCLI-D-12-00150.1.

Emanuel, K. A., 1999: The power of a hurricane: An example of reckless driving on the information superhighway. *Weather,* **54,** 107–108, doi:10.1002/j.1477-8696.1999.tb06435.x.

Emile-Geay, J., K. M. Cobb, M. E. Mann, and A. T. Wittenberg, 2013a: Estimating central equatorial Pacific SST variability over the past millennium. Part I: Methodology and validation. *J. Climate,* **26,** 2302–2328, doi:10.1175/JCLI-D-11-00510.1.

——, ——, ——, and ——, 2013b: Estimating central equatorial Pacific SST variability over the past millennium. Part II: Reconstructions and implications. *J. Climate,* **26,** 2329–2352, doi:10.1175/JCLI-D-11-00511.1.

Fedorov, A. V., S. L. Harper, S. G. Philander, B. Winter, and A. T. Wittenberg, 2003: How predictable is El Niño? *Bull. Amer. Meteor. Soc.,* **84,** 911–919, doi:10.1175/BAMS-84-7-911.

Flügel, M., and P. Chang, 1999: Stochastically induced climate shift of El Niño–Southern Oscillation. *Geophys. Res. Lett.,* **26,** 2473–2476, doi:10.1029/1999GL900550.

——, ——, and C. Penland, 2004: The role of stochastic forcing in modulating ENSO predictability. *J. Climate,* **17,** 3125–3140, doi:10.1175/1520-0442(2004)017<3125:TROSFI>2.0.CO;2.

Frankcombe, L. M., A. von der Heydt, and H. A. Dijkstra, 2010: North Atlantic multidecadal climate variability: An investigation of dominant time scales and processes. *J. Climate,* **23,** 3626–3638, doi:10.1175/2010JCLI3471.1.

Furtado, J. C., E. Di Lorenzo, N. Schneider, and N. Bond, 2011: North Pacific decadal variability and climate change in the IPCC AR4 models. *J. Climate,* **24,** 3049–3067, doi:10.1175/2010JCLI3584.1.

Galbraith, E. D., and Coauthors, 2011: Climate variability and radiocarbon in the CM2Mc Earth System Model. *J. Climate,* **24,** 4230–4254, doi:10.1175/2011JCLI3919.1.

Gebbie, G., I. Eisenman, A. Wittenberg, and E. Tziperman, 2007: Modulation of westerly wind bursts by sea surface temperature: A semistochastic feedback for ENSO. *J. Atmos. Sci.,* **64,** 3281–3295, doi:10.1175/JAS4029.1.

Gnanadesikan, A., and Coauthors, 2006: GFDL's CM2 global coupled climate models. Part II: The baseline ocean simulation. *J. Climate,* **19,** 675–697, doi:10.1175/JCLI3630.1.

Goddard, L., and M. Dilley, 2005: El Niño: Catastrophe or opportunity? *J. Climate,* **18,** 651–665, doi:10.1175/JCLI-3277.1.

——, and Coauthors, 2013: A verification framework for interannual-to-decadal predictions experiments. *Climate Dyn.,* **40,** 245–272, doi:10.1007/s00382-012-1481-2.

Griffies, S. M., and Coauthors, 2005: Formulation of an ocean model for global climate simulations. *Ocean Sci.,* **1,** 45–79, doi:10.5194/os-1-45-2005.

——, and Coauthors, 2011: GFDL's CM3 coupled climate model: Characteristics of the ocean and sea ice simulations. *J. Climate,* **24,** 3520–3544, doi:10.1175/2011JCLI3964.1.

Grötzner, A., M. Latif, A. Timmermann, and R. Voss, 1999: Interannual to decadal predictability in a coupled ocean–atmosphere general circulation model. *J. Climate,* **12,** 2607–2624, doi:10.1175/1520-0442(1999)012<2607:ITDPIA>2.0.CO;2.

Guilyardi, E., 2006: El Niño–mean state–seasonal cycle interactions in a multi-model ensemble. *Climate Dyn.,* **26,** 329–348, doi:10.1007/s00382-005-0084-6.

——, A. Wittenberg, A. Fedorov, M. Collins, C. Wang, A. Capotondi, G. J. van Oldenborgh, and T. Stockdale, 2009: Understanding El Niño in ocean–atmosphere general circulation models: Progress and challenges. *Bull. Amer. Meteor. Soc.,* **90,** 325–340, doi:10.1175/2008BAMS2387.1.

——, H. Bellenger, M. Collins, S. Ferrett, W. Cai, and A. Wittenberg, 2012a: A first look at ENSO in CMIP5. *CLIVAR Exchanges,* No. 58, International CLIVAR Project Office, Southampton, United Kingdom, 29–32.

——, W. Cai, M. Collins, A. Fedorov, F.-F. Jin, A. Kumar, D.-Z. Sun, and A. Wittenberg, 2012b: New strategies for evaluating ENSO processes in climate models. *Bull. Amer. Meteor. Soc.,* **93,** 235–238, doi:10.1175/BAMS-D-11-00106.1.

Imada, Y. and M. Kimoto, 2009: ENSO amplitude modulation related to Pacific decadal variability. *Geophys. Res. Lett.,* **36,** L03706, doi:10.1029/2008GL036421.

Jin, E. K., and Coauthors, 2008: Current status of ENSO prediction skill in coupled ocean–atmosphere models. *Climate Dyn.,* **31,** 647–664, doi:10.1007/s00382-008-0397-3.

Jochum, M. and R. Murtugudde, 2004: Internal variability of the tropical Pacific Ocean. *Geophys. Res. Lett.,* **31,** L14309, doi:10.1029/2004GL020488.

Joseph, R., and S. Nigam, 2006: ENSO evolution and teleconnections in IPCC's twentieth-century climate simulations: Realistic representation? *J. Climate,* **19,** 4360–4377, doi:10.1175/JCLI3846.1.

Karamperidou, C., M. A. Cane, U. Lall, and A. T. Wittenberg, 2013: Intrinsic modulation of ENSO predictability viewed through a local Lyapunov lens. *Climate Dyn.,* **42,** 253–270, doi:10.1007/s00382-013-1759-z.

Keenlyside, N. S., M. Latif, J. Jungclaus, L. Kornblueh, and E. Roeckner, 2008: Advancing decadal-scale climate prediction in the North Atlantic sector. *Nature,* **453,** 84–88, doi:10.1038/nature06921.

Kessler, W. S., 2002: Is ENSO a cycle or a series of events? *Geophys. Res. Lett.,* **29,** 2125, doi:10.1029/2002GL015924.

Kirtman, B. P., and P. S. Schopf, 1998: Decadal variability in ENSO predictability and prediction. *J. Climate,* **11,** 2804–2822, doi:10.1175/1520-0442(1998)011<2804:DVIEPA>2.0.CO;2.

Kleeman, R., 2008: Stochastic theories for the irregularity of ENSO. *Philos. Trans. Roy. Soc. London,* **A366,** 2509–2524, doi:10.1098/rsta.2008.0048.

——, and S. B. Power, 1994: Limits to predictability in a coupled ocean–atmosphere model due to atmospheric noise. *Tellus,* **46A,** 529–540, doi:10.1034/j.1600-0870.1994.00014.x.

Knaff, J. A., and C. W. Landsea, 1997: An El Niño–Southern Oscillation climatology and persistence (CLIPER) forecasting scheme. *Wea. Forecasting,* **12,** 633–652, doi:10.1175/1520-0434(1997)012<0633:AENOSO>2.0.CO;2.

Knutson, T. R., F. Zeng, and A. T. Wittenberg, 2013a: Multimodel assessment of regional surface temperature trends: CMIP3 and CMIP5 twentieth-century simulations. *J. Climate,* **26,** 8709–8743, doi:10.1175/JCLI-D-12-00567.1.

——, ——, and ——, 2013b: The extreme March–May 2012 warm anomaly over the eastern United States: Global context and multimodel trend analysis [in ''Explaining extreme events of 2012 from a climate perspective'']. *Bull. Amer. Meteor. Soc.,* **94** (Suppl.), S13–S17, doi:10.1175/BAMS-D-13-00085.1.

Kosaka, Y., and S.-P. Xie, 2013: Recent global-warming hiatus tied to equatorial Pacific surface cooling. *Nature,* **501,** 403–407, doi:10.1038/nature12534.

Kravtsov, S., 2012: An empirical model of decadal ENSO variability. *Climate Dyn.,* **39,** 2377–2391, doi:10.1007/s00382-012-1424-y.

Kug, J.-S., J. Choi, S.-I. An, F.-F. Jin, and A. T. Wittenberg, 2010: Warm pool and cold tongue El Niño events as simulated by the GFDL CM2.1 coupled GCM. *J. Climate,* **23,** 1226–1239, doi:10.1175/2009JCLI3293.1.

Larkin, N. K., and D. E. Harrison, 2002: ENSO warm (El Niño) and cold (La Niña) event life cycles: Ocean surface anomaly patterns, their symmetries, asymmetries, and implications. *J. Climate,* **15,** 1118–1140, doi:10.1175/1520-0442(2002)015<1118:EWENOA>2.0.CO;2.

Latif, M., and Coauthors, 1998: A review of the predictability and prediction of ENSO. *J. Geophys. Res.,* **103,** 14 375–14 393, doi:10.1029/97JC03413.

Lengaigne, M., and G. A. Vecchi, 2010: Contrasting the termination of moderate and extreme El Niño events in coupled general circulation models. *Climate Dyn.,* **35,** 299–313, doi:10.1007/s00382-009-0562-3.

Li, J., S.-P. Xie, E. R. Cook, G. Huang, R. D'Arrigo, F. Lue, J. Ma, and X.-T. Zheng, 2011: Interdecadal modulation of El Niño amplitude during the past millennium. *Nat. Climate Change,* **1,** 114–118, doi:10.1038/nclimate1086.

——, and Coauthors, 2013: El Niño modulations over the past seven centuries. *Nat. Climate Change,* **3,** 822–826, doi:10.1038/nclimate1936.

Li, Y., and N.-C. Lau, 2012: Contributions of downstream eddy development to the teleconnection between ENSO and the atmospheric circulation over the North Atlantic. *J. Climate,* **25,** 4993–5010, doi:10.1175/JCLI-D-11-00377.1.

Luo, J.-J., S. Masson, S. K. Behera, and T. Yamagata, 2008: Extended ENSO predictions using a fully coupled ocean–atmosphere model. *J. Climate,* **21,** 84–93, doi:10.1175/2007JCLI1412.1.

Mason, S. J., and G. M. Mimmack, 2002: Comparison of some statistical methods of probabilistic forecasting of ENSO. *J. Climate,* **15,** 8–29, doi:10.1175/1520-0442(2002)015<0008:COSSMO>2.0.CO;2.

Matei, D., N. Keenlyside, M. Latif, and J. Jungclaus, 2008: Subtropical forcing of tropical Pacific climate and decadal ENSO modulation. *J. Climate,* **21,** 4691–4709, doi:10.1175/2008JCLI2075.1.

McGregor, S., A. Timmermann, M. H. England, O. E. Timm, and A. T. Wittenberg, 2013: Inferred changes in El Niño–Southern Oscillation variance over the past six centuries. *Climate Past Discuss.,* **9,** 2929–2966, doi:10.5194/cpd-9-2929-2013.

McPhaden, M. J., T. Lee, and D. McClurg, 2011: El Niño and its relationship to changing background conditions in the tropical Pacific Ocean. *Geophys. Res. Lett.,* **38,** L15709, doi:10.1029/2011GL048275.

Meehl, G. A., and Coauthors, 2007: Global climate projections. *Climate Change 2007: The Physical Science Basis,* S. Solomon et al., Eds., Cambridge University Press, 747–845.

Merryfield, W. J., 2006: Changes to ENSO under CO_2 doubling in a multimodel ensemble. *J. Climate,* **19,** 4009–4027, doi:10.1175/JCLI3834.1.

Moon, B.-K., S.-W. Yeh, B. Dewitte, J.-G. Jhun, and I.-S. Kang, 2007: Source of low frequency modulation of ENSO amplitude in a CGCM. *Climate Dyn.,* **29,** 101–111, doi:10.1007/s00382-006-0219-4.

Msadek, R., K. W. Dixon, T. L. Delworth, and W. Hurlin, 2010: Assessing the predictability of the Atlantic meridional overturning circulation and associated fingerprints. *Geophys. Res. Lett.,* **37,** L19608, doi:10.1029/2010GL044517.

Newman, M., 2013: An empirical benchmark for decadal forecasts of global surface temperature anomalies. *J. Climate,* **26,** 5260–5269, doi:10.1175/JCLI-D-12-00590.1.

——, G. P. Compo, and M. A. Alexander, 2003: ENSO-forced variability of the Pacific decadal oscillation. *J. Climate,* **16,** 3853–3857, doi:10.1175/1520-0442(2003)016<3853:EVOTPD>2.0.CO;2.

——, M. A. Alexander, and J. D. Scott, 2011a: An empirical model of tropical ocean dynamics. *Climate Dyn.,* **37,** 1823–1841, doi:10.1007/s00382-011-1034-0.

——, S.-I. Shin, and M. A. Alexander, 2011b: Natural variation in ENSO flavors. *Geophys. Res. Lett.,* **38,** L14705, doi:10.1029/2011GL047658.

Ogata, T., S.-P. Xie, A. Wittenberg, and D.-Z. Sun, 2013: Interdecadal amplitude modulation of the El Niño–Southern Oscillation and its impacts on tropical Pacific decadal variability. *J. Climate,* **26,** 7280–7297, doi:10.1175/JCLI-D-12-00415.1.

Penland, C., and P. D. Sardeshmukh, 1995: The optimal growth of tropical sea surface temperature anomalies. *J. Climate,* **8,** 1999–2024, doi:10.1175/1520-0442(1995)008<1999:TOGOTS>2.0.CO;2.

——, M. Flügel, and P. Chang, 2000: Identification of dynamical regimes in an intermediate coupled ocean–atmosphere model. *J. Climate,* **13,** 2105–2115, doi:10.1175/1520-0442(2000)013<2105:IODRIA>2.0.CO;2.

Power, S., and R. Colman, 2006: Multi-year predictability in a coupled general circulation model. *Climate Dyn.,* **26,** 247–272, doi:10.1007/s00382-005-0055-y.

——, M. Haylock, R. Colman, and X. Wang, 2006: The predictability of interdecadal changes in ENSO activity and

ENSO teleconnections. *J. Climate,* **19,** 4755–4771, doi:10.1175/JCLI3868.1.

Rashid, H. A., S. B. Power, and J. R. Knight, 2010: Impact of multidecadal fluctuations in the Atlantic thermohaline circulation on Indo-Pacific climate variability in a coupled GCM. *J. Climate,* **23,** 4038–4044, doi:10.1175/2010JCLI3430.1.

Reichler, T., and J. Kim, 2008: How well do coupled models simulate today's climate? *Bull. Amer. Meteor. Soc.,* **89,** 303–311, doi:10.1175/BAMS-89-3-303.

Rodgers, K. B., P. Friederichs, and M. Latif, 2004: Tropical Pacific decadal variability and its relation to decadal modulations of ENSO. *J. Climate,* **17,** 3761–3774, doi:10.1175/1520-0442(2004)017<3761:TPDVAI>2.0.CO;2.

Sarachik, E. S., and M. A. Cane, 2010: *The El Niño–Southern Oscillation Phenomenon.* Cambridge University Press, 369 pp.

Schopf, P. S., and R. J. Burgman, 2006: A simple mechanism for ENSO residuals and asymmetry. *J. Climate,* **19,** 3167–3179, doi:10.1175/JCLI3765.1.

Smith, D. M., S. Cusack, A. W. Colman, C. K. Folland, G. R. Harris, and J. M. Murphy, 2007: Improved surface temperature prediction for the coming decade from a global climate model. *Science,* **317,** 796–799, doi:10.1126/science.1139540.

Solomon, A., and M. Newman, 2011: Decadal predictability of tropical Indo-Pacific Ocean temperature trends due to anthropogenic forcing in a coupled climate model. *Geophys. Res. Lett.*, **38,** L02703, doi:10.1029/2010GL045978.

Song, Q., G. A. Vecchi, and A. J. Rosati, 2008: Predictability of the Indian Ocean sea surface temperature anomalies in the GFDL coupled model. *Geophys. Res. Lett.,* **35,** L02701, doi:10.1029/2007GL031966.

Stevenson, S., B. Fox-Kemper, M. Jochum, R. Neale, C. Deser, and G. Meehl, 2012: Will there be a significant change to El Niño in the twenty-first century? *J. Climate,* **25,** 2129–2145, doi:10.1175/JCLI-D-11-00252.1.

Stouffer, R. J., and Coauthors, 2006: GFDL's CM2 global coupled climate models. Part IV: Idealized climate response. *J. Climate,* **19,** 723–740, doi:10.1175/JCLI3632.1.

Sun, C., M. M. Rienecker, A. Rosati, M. Harrison, A. Wittenberg, C. L. Keppenne, J. P. Jacob, and R. M. Kovach, 2007: Comparison and sensitivity of ODASI ocean analyses in the tropical Pacific. *Mon. Wea. Rev.,* **135,** 2242–2264, doi:10.1175/MWR3405.1.

Sun, D.-Z., and T. Zhang, 2006: A regulatory effect of ENSO on the time-mean thermal stratification of the equatorial upper ocean. *Geophys. Res. Lett.,* **33,** L07710, doi:10.1029/2005GL025296.

Svendsen, L., N. G. Kvamstø, and N. Keenlyside, 2013: Weakening AMOC connects equatorial Atlantic and Pacific interannual variability. *Climate Dyn.,* doi:10.1007/s00382-013-1904-8.

Takahashi, K., A. Montecinos, K. Goubanova, and B. Dewitte, 2011: ENSO regimes: Reinterpreting the canonical and Modoki El Niño. *Geophys. Res. Lett.,* **38,** L10704, doi:10.1029/2011GL047364.

Tang, Y., Z. Deng, X. Zhou, Y. Cheng, and D. Chen, 2008: Interdecadal variation of ENSO predictability in multiple models. *J. Climate,* **21,** 4811–4833, doi:10.1175/2008JCLI2193.1.

Taylor, K. E., R. J. Stouffer, and G. A. Meehl, 2012: An overview of CMIP5 and the experiment design. *Bull. Amer. Meteor. Soc.,* **93,** 485–498, doi:10.1175/BAMS-D-11-00094.1.

Timmermann, A., F.-F. Jin, and J. Abshagen, 2003: A nonlinear theory for El Niño bursting. *J. Atmos. Sci.,* **60,** 152–165, doi:10.1175/1520-0469(2003)060<0152:ANTFEN>2.0.CO;2.

——, and Coauthors, 2007: The influence of a weakening of the Atlantic meridional overturning circulation on ENSO. *J. Climate,* **20,** 4899–4919, doi:10.1175/JCLI4283.1.

Ting, M., Y. Kushnir, R. Seager, and C. Li, 2011: Robust features of Atlantic multi-decadal variability and its climate impacts. *Geophys. Res. Lett.,* **38,** L17705, doi:10.1029/2011GL048712.

van Oldenborgh, G. J., S. Y. Philip, and M. Collins, 2005: El Niño in a changing climate: A multi-model study. *Ocean Sci.,* **1,** 81–95, doi:10.5194/os-1-81-2005.

Vecchi, G. A., 2006: The termination of the 1997–98 El Niño. Part II: Mechanisms of atmospheric change. *J. Climate,* **19,** 2647–2664, doi:10.1175/JCLI3780.1.

——, and D. E. Harrison, 2006: The termination of the 1997–98 El Niño. Part I: Mechanisms of oceanic change. *J. Climate,* **19,** 2633–2646, doi:10.1175/JCLI3776.1.

——, and A. T. Wittenberg, 2010: El Niño and our future climate: Where do we stand? *Wiley Interdiscip. Rev.: Climate Change,* **1,** 260–270, doi:10.1002/wcc.33.

——, B. J. Soden, A. T. Wittenberg, I. M. Held, A. Leetmaa, and M. J. Harrison, 2006a: Weakening of tropical Pacific atmospheric circulation due to anthropogenic forcing. *Nature,* **441,** 73–76, doi:10.1038/nature04744.

——, A. T. Wittenberg, and A. Rosati, 2006b: Reassessing the role of stochastic forcing in the 1997–1998 El Niño. *Geophys. Res. Lett.,* **33,** L01706, doi:10.1029/2005GL024738.

——, and Coauthors, 2013: Multiyear predictions of North Atlantic hurricane frequency: Promise and limitations. *J. Climate,* **26,** 5337–5357, doi:10.1175/JCLI-D-12-00464.1.

Wang, B., 1995: Interdecadal changes in El Niño onset in the last four decades. *J. Climate,* **8,** 267–285, doi:10.1175/1520-0442(1995)008<0267:ICIENO>2.0.CO;2.

——, and S.-I. An, 2001: Why the properties of El Niño changed during the late 1970s. *Geophys. Res. Lett.,* **28,** 3709–3712, doi:10.1029/2001GL012862.

——, and ——, 2002: A mechanism for decadal changes of ENSO behavior: Roles of background wind changes. *Climate Dyn.,* **18,** 475–486, doi:10.1007/s00382-001-0189-5.

——, and Coauthors, 2008: Advance and prospectus of seasonal prediction: Assessment of the APCC/CliPAS 14-model ensemble retrospective seasonal prediction (1980–2004). *Climate Dyn.,* **33,** 93–117, doi:10.1007/s00382-008-0460-0.

Wang, G., R. Kleeman, N. Smith, and F. Tseitkin, 2002: The BMRC coupled general circulation model ENSO forecast system. *Mon. Wea. Rev.,* **130,** 975–991, doi:10.1175/1520-0493(2002)130<0975:TBCGCM>2.0.CO;2.

Watanabe, M., and A. T. Wittenberg, 2012: A method for disentangling El Niño–mean state interaction. *Geophys. Res. Lett.,* **39,** L14702, doi:10.1029/2012GL052013.

——, J.-S. Kug, F.-F. Jin, M. Collins, M. Ohba, and A. T. Wittenberg, 2012: Uncertainty in the ENSO amplitude change from the past to the future. *Geophys. Res. Lett.,* **39,** L20703, doi:10.1029/2012GL053305.

Wittenberg, A. T., 2002: ENSO response to altered climates. Ph.D. dissertation, Princeton University, 320 pp. [Available online at http://gfdl.noaa.gov/~atw/research/thesis/color.pdf.]

——, 2004: Extended wind stress analyses for ENSO. *J. Climate,* **17,** 2526–2540, doi:10.1175/1520-0442(2004)017<2526:EWSAFE>2.0.CO;2.

——, 2009: Are historical records sufficient to constrain ENSO simulations? *Geophys. Res. Lett.,* **36,** L14709, doi:10.1029/2009GL038710.

——, A. Rosati, N.-C. Lau, and J. J. Ploshay, 2006: GFDL's CM2 global coupled climate models. Part III: Tropical Pacific climate and ENSO. *J. Climate,* **19,** 698–722, doi:10.1175/JCLI3631.1.

Xie, S.-P., C. Deser, G. A. Vecchi, J. Ma, H. Teng, and A. T. Wittenberg, 2010: Global warming pattern formation: Sea surface temperature and rainfall. *J. Climate,* **23,** 966–986, doi:10.1175/2009JCLI3329.1.

Yang, X., and Coauthors, 2013: A predictable AMO-like pattern in GFDL's fully coupled ensemble initialization and decadal forecasting system. *J. Climate,* **26,** 650–661, doi:10.1175/JCLI-D-12-00231.1.

Yeh, S.-W., and B. P. Kirtman, 2005: Pacific decadal variability and decadal ENSO amplitude modulation. *Geophys. Res. Lett.,* **32,** L05703, doi:10.1029/2004GL021731.

——, J.-G. Jhun, I.-S. Kang, and B. P. Kirtman, 2004: The decadal ENSO variability in a hybrid coupled model. *J. Climate,* **17,** 1225–1238, doi:10.1175/1520-0442(2004)017<1225:TDEVIA>2.0.CO;2.

——, J.-S. Kug, B. Dewitte, M.-H. Kwon, B. P. Kirtman, and F.-F. Jin, 2009: El Niño in a changing climate. *Nature,* **461,** 511–514, doi:10.1038/nature08316.

Yukimoto, S., and Y. Kitamura, 2003: An investigation of the irregularity of El Niño in a coupled GCM. *J. Meteor. Soc. Japan,* **81,** 599–622, doi:10.2151/jmsj.81.599.

Zavala-Garay, J., C. Zhang, A. M. Moore, A. T. Wittenberg, M. J. Harrison, A. Rosati, J. Vialard, and R. Kleeman, 2008: Sensitivity of hybrid ENSO models to unresolved atmospheric variability. *J. Climate,* **21,** 3704–3721, doi:10.1175/2007JCLI1188.1.

Zhang, C., H. H. Hendon, W. S. Kessler, and A. J. Rosati, 2001: A workshop on the MJO and ENSO. *Bull. Amer. Meteor. Soc.,* **82,** 971–976, doi:10.1175/1520-0477(2001)082<0971:MSAWOT>2.3.CO;2.

Zhang, D., R. Msadek, M. J. McPhaden, and T. Delworth, 2011: Multidecadal variability of the North Brazil Current and its connection to the Atlantic meridional overturning circulation. *J. Geophys. Res.,* **116,** C04012, doi:10.1029/2010JC006812.

Zhang, L., and C. Wang, 2013: Multidecadal North Atlantic sea surface temperature and Atlantic meridional overturning circulation variability in CMIP5 historical simulations. *J. Geophys. Res.,* **118,** 5772–5791, doi:10.1002/jgrc.20390.

——, M. Flügel, and P. Chang, 2003: Testing the stochastic mechanism for low-frequency variations in ENSO predictability. *Geophys. Res. Lett.,* **30,** 1630, doi:10.1029/2003GL017505.

Zhang, R., and T. L. Delworth, 2005: Simulated tropical response to a substantial weakening of the Atlantic thermohaline circulation. *J. Climate,* **18,** 1853–1860, doi:10.1175/JCLI3460.1.

——, and D. G. DeWitt, 2006: Response of tropical Pacific interannual variability to decadal entrainment temperature change in a hybrid coupled model. *Geophys. Res. Lett.,* **33,** L08611, doi:10.1029/2005GL025286.

——, and Coauthors, 2013: Have aerosols caused the observed Atlantic multidecadal variability? *J. Atmos. Sci.,* **70,** 1135–1144, doi:10.1175/JAS-D-12-0331.1.

Zhang, S., M. J. Harrison, A. T. Wittenberg, A. Rosati, J. L. Anderson, and V. Balaji, 2005: Initialization of an ENSO forecast system using a parallelized ensemble filter. *Mon. Wea. Rev.,* **133,** 3176–3201, doi:10.1175/MWR3024.1.

——, ——, A. Rosati, and A. Wittenberg, 2007: System design and evaluation of coupled ensemble data assimilation for global oceanic climate studies. *Mon. Wea. Rev.,* **135,** 3541–3564, doi:10.1175/MWR3466.1.